Total and methyl-mercury seasonal particulate fluxes in the water column of a large lake (Lake Geneva, Switzerland)

Gascon Diez, Elena; Graham, Neil; Loizeau, Jean-Luc

How to cite

GASCON DIEZ, Elena, GRAHAM, Neil, LOIZEAU, Jean-Luc. Total and methyl-mercury seasonal particulate fluxes in the water column of a large lake (Lake Geneva, Switzerland). In: Environmental Science and Pollution Research, 2018. doi: 10.1007/s11356-018-2252-3

This publication URL: https://archive-ouverte.unige.ch/unige:104611
Publication DOI: 10.1007/s11356-018-2252-3

Authors post-print, Environmental Science and Pollution Research, Vol. XX, XX-XX, 2018
DOI:10.1007/s11356-018-2252-3; published online: 16 May 2018

Total and methyl-mercury seasonal particulate fluxes in the water column of a large lake (Lake Geneva, Switzerland)

Elena Gascón Díez*, Neil D Graham‡, Jean-Luc Loizeau

Abstract
Concentrations and fluxes of total and methylmercury were determined in surface sediments and associated with settling particles at two sites in Lake Geneva to evaluate the sources and dynamics of this toxic contaminant. Total mercury concentrations measured in settling particles were different throughout the seasons, and were greatly influenced by the Rhone River particulate inputs. Total mercury concentrations closer to shore (NG2) ranged between 0.073 ± 0.001 and 0.27 ± 0.01 μg/g and between 0.038 ± 0.001 and 0.214 ± 0.008 μg/g at a site deeper in the lake (NG3). Total mercury fluxes ranged between 0.144 ± 0.002 and 3.0 ± 0.1 μg/m^2/day at NG2, and between 0.102 ± 0.008 and 1.32 ± 0.08 μg/m^2/day at NG3. Combined results of concentrations and fluxes showed that total mercury concentrations in settling particles are related to the season and particle inputs from the Rhone River. Despite an observed decrease in total mercury fluxes from the coastal zone towards the open lake, NG3 (~3 km from the shoreline) was still affected by the coastal boundary, as compared to distal sites at the center of the lake. Thus, sediment focusing is not efficient enough to redistribute contaminant inputs originating from the coastal zones, to the lake center. Methylmercury concentrations in settling particles largely exceeded the concentrations found in sediments, and their fluxes did not show significant differences with relation to the distance from shore. The methylmercury found associated with settling particles would be related to the lake's internal production rather than the effect of transport from sediment resuspension.

Keywords
Mercury fluxes, mercury transport, settling particles, methylmercury, Lake Geneva, freshwater pollution, sediment traps.

Department F.-A. Forel for Environmental and Aquatic Sciences, and Institute for Environmental Sciences, University of Geneva, Boulevard Carl-Vogt 66, 1211 Geneva 4, Switzerland
‡ present adress: *Soil & Water Research Infrastructure, Biology Centre, Czech Academy of Sciences, Na Sádkách 7, České Budějovice 370 05, Czech Republic*
***Corresponding author**: Elena.Gascon@unige.ch

1. Introduction

Mercury (Hg) fate in aquatic environments is mainly related to organic and inorganic particle transport, deposition, and resuspension, as well as biologically driven transformation such as methylation and demethylation. In the atmosphere, it is essentially found as elemental Hg. Due to the relative insolubility of gaseous Hg, this trace metal is readily transported through the atmosphere and is subject to dry and wet deposition to aquatic systems (Mason et al. 2012). This atmospheric source is in addition to the Hg directly released into aquatic environments through industrial and domestic effluents, or indirectly via surface run-off and soil erosion (Kocman et al. 2017). Once in the water column, Hg primarily adsorbs onto particulate organic matter (OM) and inorganic particles and eventually settles to the sediment surface. Therefore, sediments are the principal reservoir of Hg in aquatic systems (Benoit et al. 1998; Wang et al. 1998). Methylmercury (MeHg) is a neurotoxin and one of the most hazardous forms of Hg. It accumulates in aquatic organisms and bioamplifies through the food chain posing a threat to human health from its uptake via fish consumption. Methylmercury results from the biotransformation of inorganic Hg in suboxic sediments by specific anaerobic microorganisms, including sulfate-reducing bacteria (SRB), iron-reducing bacteria (IRB) and methanogens (Compeau and Bartha 1984; Korthals and Winfrey 1987; Parks et al. 2013; Gilmour et al. 2013; Podar et al. 2015). In turn, sediments can be an important significant source of Hg to the water column depending on the biogeochemical and transport processes taking place in both sediments and waters. (Gagnon et al. 1997; Rigaud et al. 2013). Although many studies on trace metals have focused on Hg fluxes at the sediment-water interface over short periods of time (e.g. Bloom et al. 1999; Rolfhus et al. 2003; Mason et al. 2006; Feyte et al. 2012), less attention has been paid to particle-bound Hg settling fluxes and the effects of resuspension on the fate of Hg over longer periods of time. It has been shown that sediment resuspension

plays a role in Hg methylation and in MeHg transfer from sediments to organisms in shallow aquatic systems (Kim et al. 2006). However, resuspension is not restricted to shallow waters and can occur when current-induced bottom shear stress exceeds the cohesive, electrostatic force between particles in surface sediments (Taylor and Birch 2000). In some cases, depending on the lake hydrodynamics, resuspended material can constitute the dominant source for particle fluxes (Evans 1994). Resuspension of sediments is an important process enabling the redistribution of particulate material and associated contaminants. Particles are the principal vector for trace metal transport; hence, the aim of this study is to understand the Hg particle-bound dynamics and fate in a large deep lake. While many studies estimated Hg flux to the sediment trough sediment core analyses (e.g. Drevnick et al. 2010; Wiklund et al. 2017) or inferred them using models (e.g. Ethier et al 2012), to our knowledge very few studies measured Hg settling fluxes directly within the water column (e.g Hurley et al. 1991; Marvin et al. 2007).

In this study, monthly concentrations and fluxes of Hg bound to settling particles were recorded in sediment traps in Lake Geneva. Together with sedimentological parameters (grain size, organic matter and carbonate content), they were used to assess the dispersion of particle-bound pollutants and to quantify the relative importance of transport processes such as direct settling, resuspension, and lateral advection. Since Hg can be associated both on the surface and incorporated within sediments and settling particles, the authors have simplified the following article by referring to both THg and MeHg as being "in" the suspended particles and sediments.

2. Materials and methods

2.1 Study site

Lake Geneva is a warm monomictic peri-alpine lake located on the border between Switzerland and France (Fig. 1). It has a surface area of 580 km^2, a maximal depth of 309 m, and a volume of 89 km^3. The main tributary to the lake is the Rhône River (70%) with a mean discharge of 185 m^3/s, and particle concentrations ranging from 20 to 2000 mg/L in the winter and summer, respectively (Dominik et al. 1987). This study was performed in and around Vidy Bay, which is the most contaminated part of Lake Geneva (Loizeau et al. 2017). Vidy Bay is affected by treated and untreated (overflows) domestic and industrial wastewaters released by the wastewater treatment plant (WWTP) of the city of Lausanne (e.g. Pardos et al. 2004; Poté et al. 2008; Thevenon et al. 2011; Gascón Díez et al. 2017). The WWTP discharges between 1 and 3 m^3/s of treated effluent, reaching as much as ~7 m^3/s when intense precipitation occurs (Razmi et al. 2013). In 2011, the mean total mercury (THg) concentration in the WWTP sludge was 3.8 μg/g (Burnier et al. 2011). Vidy Bay also receives some urban runoff through the Chamberonne River, and minor inputs from the Venoge River, both of which enter the lake to the west of the bay.

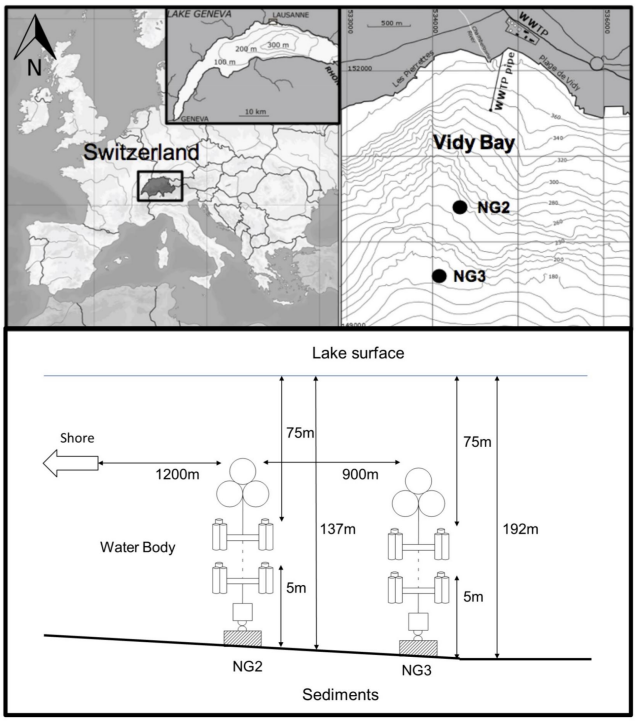

Figure 1. *Top*: Map of the study area and location of sampling stations close to Vidy Bay as related to Lake Geneva in Switzerland. Isolines corresponded to the lake bottom's altitude above sea level (a.s.l.), where the lake's surface is at 372 m a.s.l. *Bottom*: Scheme of the chain of traps deployed at NG1 and NG2 (not to scale).

2.2 Sediment and settling particles sampling

Sediment traps were deployed on a monthly basis between December 2009 and September 2011 from the Department F.-A. Forel for Environmental and Aquatic Sciences' research vessel, "La Licorne". The traps were deployed at two locations, NG2 (6°35'00" E, 46°30'06" N; Swiss coordinates: 534350 E, 150400 N) at 138 m water depth, and NG3 (6°34'46" E, 46°29'40" N; Swiss coordinates: 534050 E, 149600 N) at 192 m water depth (Fig. 1). Sediment traps consisted of a weight, an acoustic release, two tiers of sediment trap tubes, and buoys (Fig. 1). Each tier of sediment traps consisted of a frame holding six 80 x 11 cm plastic tubes, resulting in a total surface area of 570 cm2. At each location, one tier was placed at 5 m above the sediment surface while the other was placed 75 m below the lake surface.

Surface sediments below the traps were sampled at the same time and on the same frequency as the sediment traps using two Mortimer-Jenkin-type gravity corers attached together. The top 1st cm centimeter of sediment was subsampled by extrusion. Additionally, the oxidized surface sediments (approximately 1 cm depth) were collected using a Van Veen grab sampler at 15 additional sites (numbered EG1 - EG15) along a transect extending from Vidy Bay towards the deeper main basin (Fig. 2). A 60-cm long sediment core was also retrieved at NG2 on May 14th, 2014, using a UWITEC® gravity corer.

This core was used to date sediments and determine recent sediment accumulation rates.

2.3 Geochemical analyses

Sediment grain-size distribution was determined on wet sediments using a laser diffraction analyzer (Coulter LS-100, Beckman-Coulter, USA), following the procedure described by Loizeau et al. (1994). No treatment to break aggregates, dissolve carbonates or remove organic matter was performed, ensuring that the in-situ grain size was preserved.

Samples were freeze-dried in a CHRIST BETA 1-8 K freeze-drying unit (-54°C, 6 Pa) for a minimum of 48 h. Organic matter and calcium carbonate ($CaCO_3$) contents in sediments were estimated by Loss on Ignition. Samples were heated to 550°C for 30 minutes to estimate the OM mass loss and then heated to 1000°C for another 30 minutes to estimate the $CaCO_3$ content (Dean 1974). The $CaCO_3$ content was calculated by multiplying the mass loss at 1000°C by 2.2742, the molar mass ratio of calcite to carbon dioxide.

Total Hg in dry sediment was analyzed by Cold Vapor Atomic Absorption Spectrophotometry (CVAAS) using an automatic Hg analyzer, AMA-254 (Altec, ČR), following the procedure described by Roos-Barraclough et al. (2002). All analyses were conducted in triplicate. The detection limit and working range were 0.01 ng and 0.05–600 ng, respectively. Concentrations obtained for repeated analyses of the certified reference material never exceeded the specified acceptance range given for the MESS-3 reference material (National Research Council of Canada).

Methylmercury in solid matrix was extracted using a HNO_3 leaching/CH_2Cl_2 extraction method (Liu et al. 2012) followed by ethylation onto Tenax traps. The recovery of extractions and analyses of the certified reference material (ERM-CC580) were consistently above 85%. Gas chromatography separation (Bloom 1989) and Cold Vapor Atomic Fluorescence Spectrometry (CV-AFS) detection were run using a Merx Model III CV-AFS Detector (Brooks Rand, USA) with a manufacturer certified accuracy of 109% and precision of 3%.

2.4 Sediment dating and Hg flux in sediments at NG2

To determine the long-term Hg flux to the sediments, a 60-cm long sediment core was retrieved and split lengthwise. Water content and porosity were measured following the method of Håkanson and Jansson (1983). Depth scale was converted to mass scale in order to estimate sediment accumulation rates (SAR) expressed in g/m^2/day, which are independent of the change in porosity induced by compaction (see e.g. Baskaran et al. 2015 for equations). Three SARs were estimated using the following time markers: i) first occurrence of ^{137}Cs atmospheric fallout from nuclear weapon testing in 1954, assuming no ^{137}Cs redistribution within the sediments; ii) ^{137}Cs fallout maximum in 1964 from atmospheric nuclear weapon testing; iii) ^{137}Cs fallout peak from the 1986 Chernobyl accident; and iv) the surface sediment in 2014. ^{137}Cs activities were

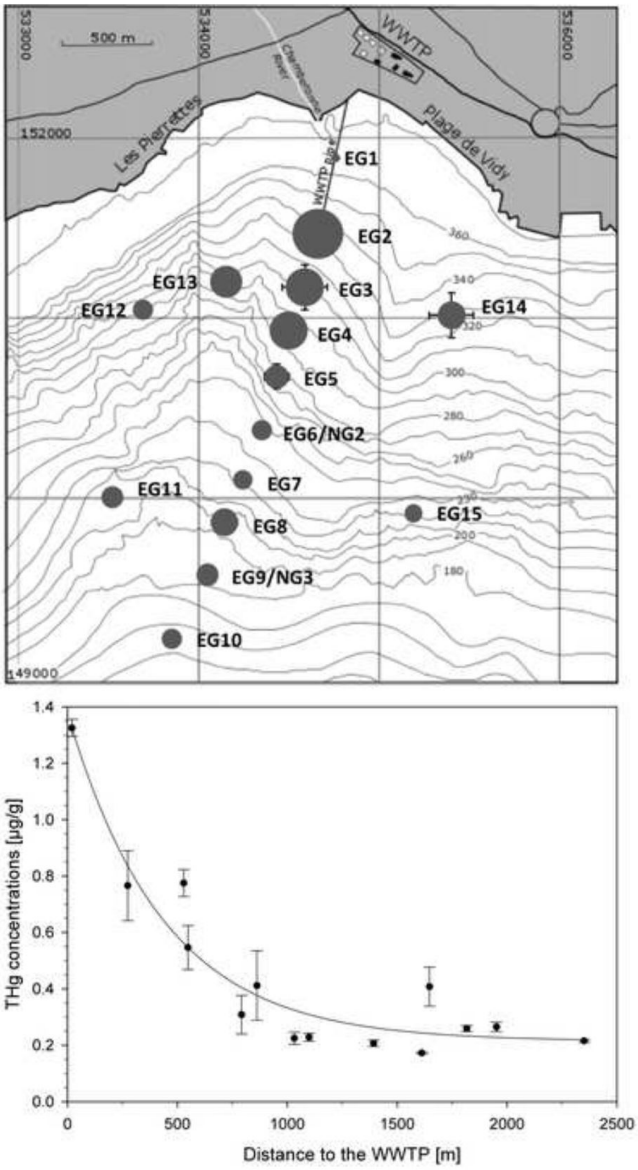

Figure 2. *Top*: Spatial variability of THg concentration in surface sediments in Vidy Bay and surrounding area. The surface area of each circle is proportional to THg content. Error bars correspond to one standard deviation determined from triplicate measurements. *Bottom*: Total Hg concentrations as a function of the distance to the WWTP outlet pipe.

measured in freeze-dried and homogenized sediment samples using an HPGe gamma spectrometer (Ortec EG&G).
Total Hg and MeHg fluxes to the surface sediments at NG2 for the period from December 2009 to September 2011 were estimated by multiplying the youngest SAR estimated in the 60-cm sediment core by the THg or MeHg mean concentration of the surface sediments for this period (2009-2011).
Fluxes are expressed in $\mu g/m^2/day$ and $ng/m^2/day$ for THg and MeHg, respectively.

2.5 Statistical analyses

Data normality was tested using a Shapiro-Wilk test. Total Hg and MeHg concentration datasets did not follow a normal distribution in top and bottom sediment traps. Therefore, median values were used to compare groups, and Kruskal-Wallis H-test (one-way analysis on ranks) was performed to compare THg concentration and fluxes in top and bottom sediment traps in autumn, summer, spring, and winter. The significance level was set to 0.05. All statistical analyses were performed with SigmaPlot® 11.0 software.

3. Results

3.1 Grain-size distribution evolution

Temporal variations in mean grain size of settling particles are illustrated in (Fig. 3) for both sites. Mean grain size varied between 14 and 48 μm. Trends were similar between NG2 and NG3, as well as between top and bottom traps. However, lower values were recorded in 2010 compared to 2011. Moreover, minimum values were found in both top and bottom traps, from the summer to autumn of 2010, and in autumn of 2011. These low values correspond to high particle fluxes, including OM and $CaCO_3$, determined in the same samples by Graham et al. (2016). In contrast, 2011 showed its highest values during spring-early summer at both sites.

3.2 Sediment core dating at NG2

The first occurrence of ^{137}Cs was measured at a mass depth of 10.15 g/cm^2, with the peak from atmospheric nuclear weapons testing at 8.17 g/cm^2, and the maximum fallout from the Chernobyl accident at 5.03 g/cm^2. From these mass depths and the elapsed time between each time marker, three mean SARs were determined: 5.42 ± 0.38 $g/m^2/day$ between 1954 and 1964; 3.83 ± 0.25 $g/m^2/day$ between 1964 - 1986; and 4.93 ± 0.36 $g/m^2/day$ between 1986 - 2014. It should be noted that the lower SAR between 1964 and 1986 has been observed over a large part of the Eastern end of the lake (T. Silva, personal communication). The most recent SAR calculated at NG2 was used to estimate the THg fluxes to the sediment and corresponds to a mean daily flux of 4.93 ± 0.36 $g/m^2/day$.

3.3 Total Hg concentrations and fluxes in surface sediments and settling particles

Total Hg concentrations were measured in the surface sediments of fifteen sites in and around Vidy Bay. Ten of these

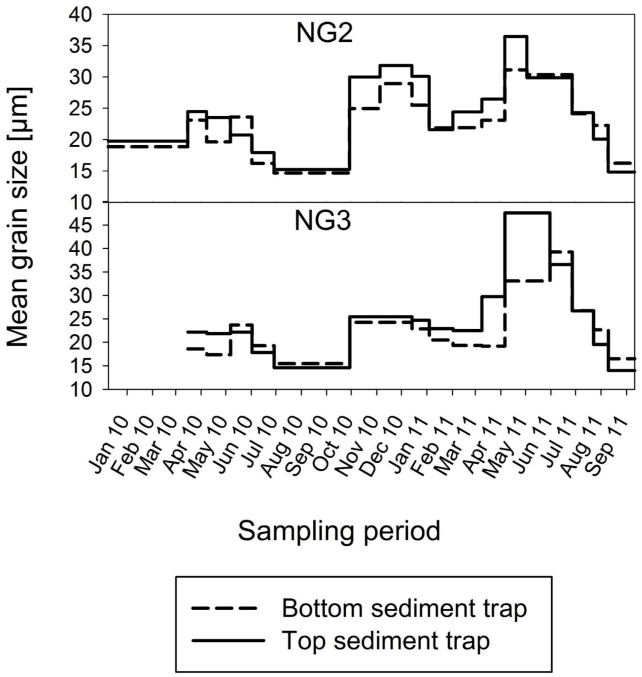

Figure 3. Mean grain size distribution of settling particles at NG2 and NG3. Solid line: top sediment trap. Dashed line: bottom sediment trap.

sites were located on a north-south transect passing along the WWTP outlet pipe, which is located between sampling sites EG1 and EG2 (Fig. 2) , upslope of the outlet pipe, had the lowest concentration of THg (0.039 ± 0.001 $\mu g/g$) whereas EG2, located approximately 20 m in front of the outlet pipe, registered the maximal concentration of 1.33 ± 0.03 $\mu g/g$. Moving away from the outlet pipe, concentrations fell between EG2 and EG6, where they plateaued at around 0.2 $\mu g/g$ (Fig. 2b). At NG2 and NG3, median THg concentrations measured in settling particles were 0.154 $\mu g/g$ and 0.097 $\mu g/g$, respectively, showing that they are not directly affected by the WWTP effluent. Total Hg concentrations measured on particles recovered in both the top and bottom sediment traps ranged between 0.073 ± 0.001 and 0.27 ± 0.01 $\mu g/g$ at NG2, and between 0.038 ± 0.001 and 0.214 ± 0.008 $\mu g/g$ at NG3. The seasonal evolution was similar at both sites and at both depths (Fig. 4). The highest THg concentrations were found in autumn-early winter, the lowest ones in summer-early autumn, and intermediate values in spring. Although seasonal variations followed the same trend at both locations, settling particles had significantly higher THg concentrations at both depths of NG2 as compared to NG3. Particularly in autumn-early winter THg concentrations in settling particles at NG2 were above the median concentration measured in sediments, whereas at NG3, THg concentrations were always lower in settling particles than in the median concentration of sediments (Fig. 4; Table SI1).
Total Hg fluxes were calculated to further understand the seasonal THg dynamics (Fig. 4, Table SI1). Total Hg fluxes

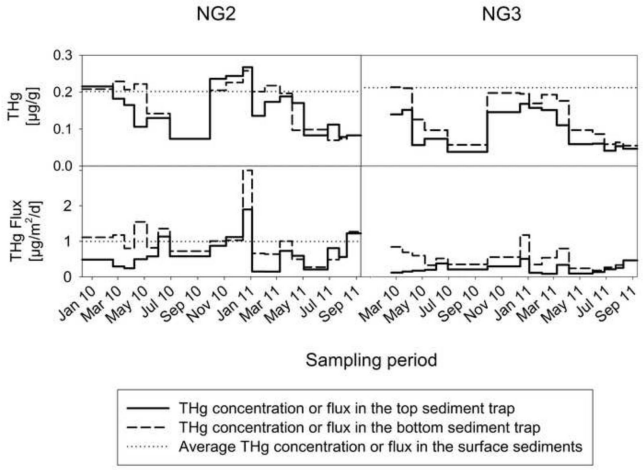

Figure 4. Total Hg THg concentrations and fluxes in settling particles and sediments at NG2 and NG3. Solid line: top sediment trap. Dashed line: bottom sediment trap. Dotted line: mean THg concentration or flux in surface sediments during the entire period of sampling.

ranged between 0.144 ± 0.002 and 3.00 ± 0.10 μg/m^2/day at NG2, and between 0.102 ± 0.008 and 1.32 ± 0.08 μg/m^2/day at NG3. At both sites, THg fluxes were usually greater in the bottom trap than in the top trap (Fig. 4). The fluxes in December 2010 were atypically high for the bottom trap of both sites, particularly at NG2 (3.00 ± 0.03 μg/m^2/day at NG2 and 1.31 ± 0.06 μg/m^2/day at NG3).

The THg flux in surface sediments at NG2 was estimated from the recent SAR determined in the 60-cm sediment core. The mean THg concentration in the surface sediment from the period December 2009 to September 2011 was 0.20 ± 0.02 μg/g, and the resulting mean THg daily flux was 0.99 ± 0.13 μg/m^2/day for that period.

The SAR to surface sediments at NG3 was not determined in this study. However, the SAR in a core located at 1365 m to the southwest from NG3 was 4.93 ± 0.55 μg/m^2/day (Loizeau et al. 2012), like the SAR obtained at NG2. Thus, we assume that the SAR at NG3 would be similar to 4.93 μg/m^2/day. The mean THg concentration in NG3 surface sediments was 0.21 ± 0.03 μg/g, resulting a mean daily THg flux of 1.04 ± 0.19 μg/m^2/day, which is comparable to that of NG2.

3.4 Methylmercury concentrations and fluxes

The median MeHg concentration in sediments was 0.84 ng/g at NG2 and 0.75 ng/g at NG3. In both top and bottom sediment traps they ranged from 0.41 ± 0.04 ng/g to 11.4 ± 0.1 ng/g with a median of 2.55 ng/g at NG2; and between 0.39 ± 0.02 ng/g and 13.5 ± 0.2 ng/g with a median of 2.17 ng/g at NG3 (Fig. 5; Table SI2). The seasonal evolution of MeHg concentrations in settling particles at NG2 showed that in 2010, the highest concentrations were found in November in the bottom trap; and contrary to THg concentrations, MeHg content in the summer-autumn of 2010 and 2011 were elevated and generally greater in the top trap. Methylmercury concentrations in settling particles were largely above the average concentration measured in sediments (Fig. 5).

NG3 showed lower concentrations between late autumn and early summer and higher concentrations between the summer and early autumn. During the latter period, MeHg concentrations in sediments traps were notably higher than the mean MeHg concentration in the surface sediments (0.78 ng/g), especially those of the bottom trap which were almost continuously greater than those of the top trap. Methylmercury fluxes in settling particles varied between 0.44 ± 0.04 ng/m^2/day and 68 ± 8 ng/m^2/day at NG2, and between 0.68 ± 0.01 ng/m^2/day and 58.5 ± 0.2 ng/m^2/day at NG3. Median values were 9.81 ng/m^2/day and 10.7 ng/m^2/day, respectively. As shown in Fig. 5, trends of MeHg fluxes at both sites were similar to concentration trends, that is, greater fluxes of MeHg in the summer and autumn as compared to winter and spring. Finally, likewise to the MeHg concentrations, MeHg fluxes measured in the bottom trap, especially at NG3, were greater than those measured in the top trap.

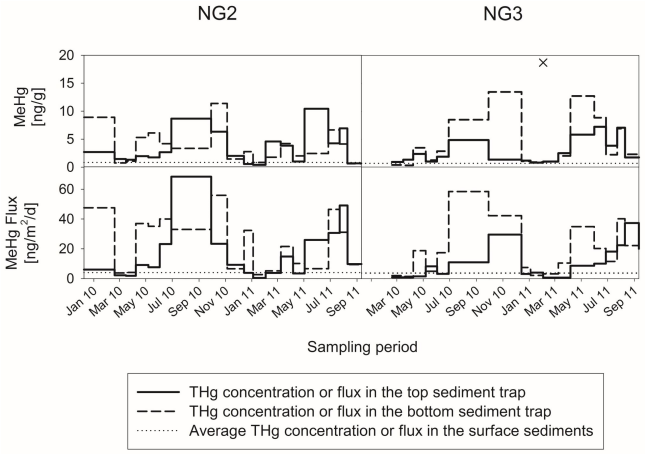

Figure 5. Methylmercury concentrations and fluxes in settling particles at NG2 and NG3. Solid line: top sediment trap. Dashed line: bottom sediment trap.

4. Discussion

4.1 Grain-size distribution

Settling particles with smaller mean grain sizes were found during the summer of 2010 and September 2011 at NG2 and NG3 (Fig. 3), corresponding to the highest fluxes of particles, but also of OM and $CaCO_3$ (Graham et al. 2016). This suggests that settling particles during these periods predominantly originated from the Rhone River's suspended load that is at its maximum during this period of the year, combined with inputs from the aggregation and settling of endogenic $CaCO_3$crystals and fine particulate OM (Gascón Díez et al. 2016). The Rhone River is the major tributary of the lake in term of discharge (about 70%) and sediment load (80%). The distribution of finer sized particles delivered by the Rhone River has previously been shown in spatial mapping of the grain-size distribu-

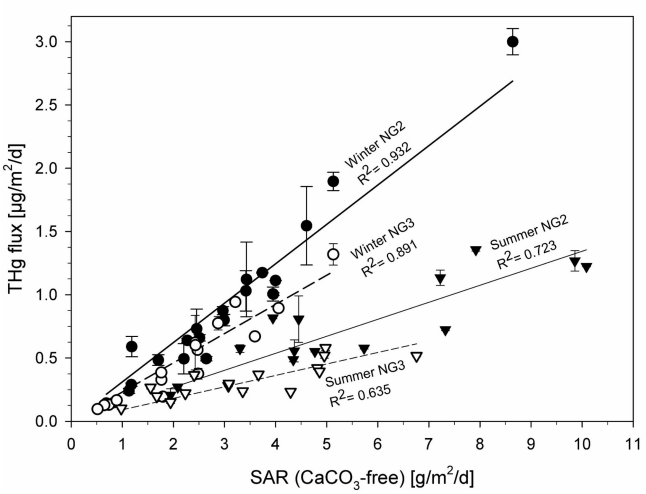

Figure 6. Linear correlations between THg flux and $CaCO_3$-free SAR at each sampling site. Black circles: winter (October to April) at NG2. White circles: winter (October to April) at NG3. Black triangles: summer (May to September) at NG2. White triangles: summer (May to September) at NG3.

tion of Lake Geneva surface sediments (Loizeau et al. 2017).

4.2 The influence of the watershed on total Hg load and seasonal trends

Many sampling sites were required to assess the THg distribution in Vidy Bay due to the high spatial heterogeneity of THg concentrations (Poté et al. 2008; Gascón Díez et al. 2013) in surface sediments of this region (Fig. 2). EG1 was the closest point to the shore and showed the lowest concentration measured in the bay (0.039 μg/g). Since Hg features a strong affinity for small organic material, the low concentrations found at EG1 is explained by the dominance of coarse-grained (sandy) sediments discharged either by the Chamberonne River, or as a result of the high-energy nature of this erosional zone that disfavors the permanent deposition of fine particles (Håkanson 1977). Hg sorption depends on the physico-chemical characteristics of sediments such as the composition, the electrostatic forces and the particle size. Thus, Hg adsorbs more readily to the 0-200 μm sediment fraction (Bengtsson and Picado 2008). EG2, at about 20 m distance from the outlet pipe, showed to be the most highly affected site in the bay with the highest THg concentration (Fig. 2). Concentrations decreased from EG2 towards the main basin, reaching a concentration plateau (0.2 μg/g) between EG7 to EG10, where concentrations were similar to those previously recorded for the center of the lake (0.17 μg/g). This suggests that the impact of the WWTP rapidly diminishes with distance, which is in agreement with previous studies (Poté et al. 2008; Bravo et al. 2011; Gascón Díez et al. 2013). Concentration data alone was not enough to fully understand the dynamics of THg associated with particles since variations in SAR may modify the particulate THg signal by dilution with uncontaminated particles. Analysis of variance of the median THg concentration values showed statistically significant differences in THg concentrations in settling particles throughout the seasons at NG2 and NG3 ($p < 0.05$). In turn, variability in the median values for the THg fluxes were not statistically significant ($p > 0.05$), inferring that the concentrations of THg were strongly influenced by the seasonal trends of SAR.

4.2.1 The main external particle input: the Rhone River

To eliminate the influence of endogenic carbonate production, carbonate-free SARs were calculated and compared with THg fluxes (Fig. 6). This scatter plot clearly shows linear correlations between the two parameters, with a strong seasonal influence, and a small but consistent influence from site location. The linear relationship in "winter" (October to April) gives a THg concentration on the carbonate-free particles of 0.31 μg/g and 0.23 μg/g at NG2 and NG3, respectively. In "summer" (May to September), these values decrease respectively to 0.14 and 0.09 μg/g. This strong seasonal variation is certainly due to the massive input of suspended particles from the Rhone River during this period; whereas in "winter", particles originate from the entire watershed. In 2010, data from the Swiss Federal Office for the Environment (OFEV, 2016) show that 89 % of the Rhone River particle load (802'000 t) was discharged to the lake between May and September. The influence of Rhone River suspended particle sedimentation on the spatial distribution of THg concentrations over the entire lake is emphasized by low (< 0.2 μg/g) THg concentrations over the Eastern part of the lake which rises to values above 0.2 μg/g over the rest of the lake with some regions presenting values greater than 0.4 μg/g (Loizeau et al. 2017). Therefore, there is strong evidence that the seasonal evolution of THg concentrations (as well as SAR) is highly influenced by the Rhone River sediment dynamics, even at great distances ($\geq$25 km) from the mouth of the river.

4.2.2 The coastal effect versus endogenic production

Total Hg fluxes were slightly greater at NG2 than at NG3, and as NG2 is 900 m closer to shore, lateral advections at NG2 are also greater than at NG3. These lateral advections are likely due to resuspensions from shallower areas, affected by inputs from the densely anthropized northern coast watershed, hence the elevated THg fluxes at NG2. Site NG3, with lower THg fluxes, would be less affected by these coastal zone inputs. The data obtained at NG2 and NG3 were compared with previous results for equivalent depths at the center of the lake in the main basin (Table 1) (Dominik et al. 1993). Although the SAR and OM fluxes were lower at NG3 than at NG2 (similar to the THg fluxes), NG3 fluxes remained higher than those found in the center of the lake (site SHL2) (Table 1). This suggests that the OM present in the water column is from both autochthonous and allochthonous sources. Further studies on the characterization of OM would be needed to establish its origin. The differences in CaCO3 fluxes between NG2, NG3, and the center of the lake were not as marked as was for SAR,

OM and THg fluxes, suggesting that endogenic CaCO3 is a significant source of calcite to the lake (Gandais 1989). Thus, production and settling of endogenic $CaCO_3$ crystals, which are season dependent (Dominik et al. 1993), along with the large suspended particle inputs of Rhone River, act to dilute the THg signal and contribute to the low concentrations of THg found in sediment traps.

THg mean concentrations in sediments were expected to be greater at NG2 than at NG3, instead, surface sediments at both sites had comparable mean values. At NG2 the THg concentrations and fluxes to sediments were similar to those measured in settling particles; however, at NG3 the THg concentrations and estimated fluxes in sediments were higher than the ones found in settling particles. These discrepancies could be due to different factors influencing the uncertainty of 2009 to 2011 sedimentation rate calculations itself, combined with the differences in the SAR estimated from core SM9, used for site NG3, in-turn leading to a large uncertainty estimation in the THg fluxes showed here.

On the other hand, THg fluxes in the water column, associated with settling particles, showed at both sites that the deposition of THg was greater in the bottom traps than in the top traps, pointing to the likely influence of lateral advection of particles and/or sediment resuspensions at 5 m above the sediment surface (Graham et al. 2016).

Finally, the maximum SAR, OM, CaCO3 and THg fluxes measured in December 2010 were likely due to intense rainfalls between October 2010 and January 2011 which entailed huge rises in the discharge from rivers in the northern Lake Geneva watershed (see section 4.2.1, Fig. 6), as recorded in the Venoge River (Fig. SI1). According to the hydrodynamics of the studied area (Graham et al. 2016), detrital material, organic matter and particulate Hg in the terrestrial run-off and watershed inputs, could be swept along the northern shore by the predominant westerly current where they would be combined with resuspensions. A minor contribution of wet deposition related to the heavy rainfall period may also have occurred.

The catchment area dynamics pointed out in sections 4.2.1 and 4.2.2 explain the importance of the THg accumulation in the shallow areas over the deeper lake, as it has also been shown for instance in Lake Hallwil (Bloesch and Uehlinger 1986). Thus, in the present study the external inputs are dominant compared to the focusing processes themselves that have been described in the literature (cf. Blais and Kalff 1995; Fuchs et al. 2016) due to the particularity of the study site.

Another important potential source of inorganic Hg in aquatic system is the atmosphere. Hg released by industrial activities is deposited in near-urban lakes (e.g. Van Metre et al. 2011). Atmospheric depositional fluxes were not directly measured in this study; however, the average THg atmospheric fluxes estimated from Van Metre et al. (2011) and Roos-Barraclough and Shotyk 2003 were about 0.19 $\mu g/m^2$/day and 0.055 $\mu g/m^2$/day, respectively. Therefore, using these values and compared to the THg fluxes at NG2 and NG3 (0.97 and 1.04 $\mu g/m^2$/day, respectively), the Hg atmospheric deposition in Lake Geneva could account for 6 to 20% of the THg flux. Nevertheless, Hg deposition depends on the location, surface topography, and vegetation of the water body (Roos-Barraclough and Shotyk 2003), thus, further measurements in this direction would be needed to further understand the Hg dynamics in Lake Geneva.

4.3 The fate of methylmercury

Higher concentrations of MeHg were expected in sediments than in settling particles because anoxic conditions prevail in subsurface sediments while particles settled through the oxic water column (dissolved oxygen ~7 mg/L) (Savoye et al. 2015; Gascón Díez et al. 2016). However, MeHg concentrations in settling particles largely exceeded the concentrations found in sediments (Fig. 5). Analysis of variance between median values did not show statistically significant differences in MeHg concentrations in settling particles throughout the seasons at NG2 ($p > 0.05$), but it showed significant differences throughout the seasons at NG3. Moreover, the highest concentrations are recorded during the warm and mild months (Fig 5). Nevertheless, to compare MeHg settling fluxes to its production and degradation in sediments, we estimated the methylation and demethylation specific fluxes (in $\mu g/m^2$/day) in the first centimeter of the sediment surface. Considering the 0.2 $\mu g/g$ average THg concentration measured in sediments; alongside the methylation rate constant (k_m) of 0.005 day^{-1} and demethylation rate constant (k_d) of 0.3 day^{-1}, previously determined for the same settings (Gascón Díez et al. 2016); a simple steady state mass balance model shows that methylation/demethylation specific fluxes are between 2 and 3 orders of magnitude greater than the MeHg fluxes from settling particles. Thus, the input of MeHg from the settling particles to the sediments is negligible in comparison to the MeHg production and degradation cycle in the sediments.

Besides, differences in MeHg seasonal fluxes were statistically significant ($p < 0.05$) at both sites, suggesting that the seasonal trends in the SAR did not influence the seasonal behavior of MeHg concentrations showing higher production during the warmer periods. In addition, contrary to THg fluxes, MeHg fluxes did not show significant differences with relation to distance from shore. Previous studies hypothesized that the high content of fresh planktonic OM associated with settling particles create oxic-deficient microenvironments inside the aggregates promoting the activity of the heterotrophic microorganisms involved in Hg-methylation processes, such as sulfate reducing bacteria (Heimburger et al. 2010; Schartup et al. 2015; Gascón Díez et al. 2016).

New insights to Hg methylation processes in the water column suggest that MeHg resuspension and diffusion from the sediments is not the only pathway for MeHg to reach the water column and, consequently, MeHg directly produced in the water column represents an underestimated source for food web.

5. Summary

A THg dispersion pathway from the shoreline to deeper waters of Lake Geneva showed a decrease of particle-bound THg fluxes, suggesting that THg inputs from the coastal zone are a dominant source as compared to focusing processes: THg fluxes at NG2 (closer to the lake shore) were higher than at NG3. Total Hg concentrations in settling particles were different throughout the seasons, and greatly influenced by endogenic carbonate precipitates and by the Rhone River sediment inputs, whereas THg fluxes varied only marginally with the seasons. The low SARs of relatively Hg-enriched particles in winter are compensated for by the high SARs of Hg-depleted particles in summer. On the other hand, THg fluxes were observed to be higher, overall, in the bottom trap than in the top trap, indicating that sediment resuspension and/or lateral THg fluxes are more efficient near the bottom boundary of the lake.

Methylmercury concentrations and fluxes were highly variable, mainly in deeper waters, and did not follow the same trend as THg. Significantly higher MeHg concentrations were found in settling particles than in sediments, and MeHg fluxes in settling particles varied significantly throughout the seasons inferring Hg-methylation processes within the water column that is stronger during the summer period.

Acknowledgments

We would like to thank Philippe Arpagaus for his help during the sampling campaigns, in addition to “La Direction Générale de l’Environnement DGE – Inspection de la pêche” and “Canton de Vaud” for allowing us to deploy the sediment traps in Lake Geneva. The work was partially funded by SNF research grant PDFMP2-123034.

References

Baskaran M, Miller CJ, Kumar A, Andersen E, Hui J, Selegeanc JP, Creech CT, Barkach J (2015) Sediment accumulation rates and sediment dynamics using five different methods in a well constrained impoundment: Case study from Union Lake, Michigan. J Great Lakes Res 41: 607-617.

Bengtsson G, Picado F (2008) Mercury sorption to sediments: Dependence on grain size, dissolved organic carbon, and suspended bacteria. Chemosphere 73:526-531.

Benoit JM, Gilmour CC, Mason RP, Riedel GS, Riedel GF (1998) Behavior of mercury in the Patuxent River estuary. Biogeochemistry 40:249-265.

Blais JM, Kalff J (1995) The influence of lake morphometry on sediment focusing. Limnol Oceanogr 40:582-588.

Bloesch J, Uehlinger U (1986) Horizontal Sedimentation Differences in a Eutrophic Swiss Lake. Limnol Oceanogr 31:1094-1109.

Bloom N (1989) Determination of Picogram Levels of Methylmercury by Aqueous Phase Ethylation, Followed by Cryogenic Gas-Chromatography with Cold Vapor Atomic Fluorescence Detection. Can J Fish Aquat Sci 46:1131-1140.

Bloom NS, Gill GA, Cappellino S, Dobbs C, Mcshea L, Driscoll C, Mason R, Rudd J (1999) Speciation and cycling of mercury in Lavaca Bay, Texas, sediments. Environ Sci Techno. 33:7-13.

Bravo AG, Bouchet S, Amouroux D, Pote J, Dominik J (2011) Distribution of mercury and organic matter in particle-size classes in sediments contaminated by a waste water treatment plant: Vidy Bay, Lake Geneva, Switzerland. J Environ Monitor 13:974-982.

Burnier G, Jaquerod CA, Poget E, Vioget P (2011) Bilans 2011 de l’épuration vaudoise. Rapport du service des eaux, sols et assaisnissement, Etat de Vaud, 27 pp.

Compeau G, Bartha R (1984) Methylation and Demethylation of Mercury under Controlled Redox, Ph, and Salinity Conditions. Appl Environ Microb 48:1203-1207.

Dean WE (1974) Determination of carbonate and organic matter in calcareous sediments and sedimentary rocks by loss on ignition; comparison with other methods. J Sediment Res 44 :242–248.

Dominik J, Burrus D, Vernet J-P (1987) Transport of the Environmental Radionuclides in an Alpine Watershed. Earth Planet Sc Lett 84:165-180.

Dominik J, Dulinski M, Span D, Hofmann A, Favarger P-Y, Vernet J-P (1993) Transfert de matière et de radioisotopes entre l’eau et les sédiments dans le Léman. Rapp Comm int prot eaux Léman contre pollut Campagne 1992 :163-188.

Drevnik PE, Shinneman ALC, Lamborg CH, Engstrom DR, Bother MH, Oris JT (2010) Mercury fluxes to sediments of Lake Tahoe, California-Nevada. Watet Air Soil Pollut 210:399-407.

Evans RD (1994) Empirical-Evidence of the Importance of Sediment Resuspension in Lakes. Hydrobiologia 284:5-12.

Ethier, ALM, Atkinson JF, DePinto JV, Lean DRS (2012) Estimating mercury concentrations and fluxes in the water column and sediment of Lake Ontario with HERMES model. Environ Pollut 161: 335-342.

Feyte S, Gobeil C, Tessier A, Cossa D (2012) Mercury dynamics in lake sediments. Geochim Cosmochim Ac 82:92-112.

Fuchs A, Selmeczy GB, Kasprzak P, Padisák J, Casper P (2016) Coincidence of sedimentation peaks with diatom blooms, wind, and calcite precipitation measured in high resolution by a multitrap. Hydrobiologia 763:329-344.

Gagnon C, Pelletier E, Mucci A (1997) Behaviour of anthropogenic mercury in coastal marine sediments. Mar Chem 59:159-176.

Gandais V (1989) Origines et variations spatio-temporelles des flux de matière particulaire au centre du Léman. Dissertation, University of Geneva.

Gascón Díez E, Bravo AG, A Porta N, Masson M, Graham ND, Stoll S, Akhtman Y, Amouroux D, Loizeau J-L (2013) Influence of a wastewater treatment plant on mercury contamination and sediment characteristics in Vidy Bay (Lake Geneva, Switzerland). Aquat Sci 76:S21-S32.

Gascón Díez E, Loizeau J-L, Cosio C, Bouchet S, Adatte T, Amouroux D, Bravo AG (2016) Role of settling particles on mercury methylation in the oxic water column of freshwater systems. Environ Sci Technol 50:11672–11679.

Gascón Díez E, Corella JP, Adatte T, Thevenon F, Loizeau J-L (2017) High-resolution reconstruction of the 20th century history of trace metals, major elements, and organic matter in sediments in a contaminated area of Lake Geneva, Switzerland. Appl Geochem 78:1-11.

Gilmour CC, Podar M, Bullock AL, Graham AM, Brown SD, Somenahally AC, Johs A, Hurt RA, Bailey KL, Elias DA (2013) Mercury Methylation by Novel Microorganisms from New Environments. Environ Sci Technol 47:11810-11820.

Graham ND (2015) The fate of sediment-bound contaminants: a case study of Vidy Bay (Lake Geneva, Switzerland. Dissertation, University of Geneva

Graham ND, Bouffard D, Loizeau J-L (2016) The influence of bottom boundary layer hydrodynamics on sediment focusing in a contaminated bay. Environ Sci Pollut Res 23:25412-25426.

Håkanson L (1977) The influence of wind, fetch, and water depth on the distribution of sediments in Lake Vänern, Sweden. Can J Earth Sci 14:397-412.

Håkanson L, Jansson M (1983) Principles of lake sedimentology. Springer-Verlag, Berlin.

Heimburger LE, Cossa D, Marty JC, Migon C, Averty B, Dufour A, Ras J (2010) Methyl mercury distributions in relation to the presence of nano- and picophytoplankton in an oceanic water column (Ligurian Sea, North-western Mediterranean). Geochim Cosmochim Ac 74:5549-5559.

Hurley JP, Watras CJ, Bloom NS (1991) Mercury cycling in a northern Wisconsin seepage lake: the role of particulate matter in vertical transport. Water Aire Soil Pollut 56:543-551.

Kim EH, Mason RP, Porter ET, Soulen HL (2006) The impact of resuspension on sediment mercury dynamics, and methylmercury production and fate: A mesocosm study. Mar Chem 102:300- 315.

Kocman D, Wilson SJ, Amos HM, Telmer KH, Steenhuisen F, Sunderland EM, Mason RP, Outridge P, Horvat M (2017) Toward an Assessment of the Global Inventory of Present-Day Mercury Releases to Freshwater Environments. Int J Environ Res Public Health 14:138.

Korthals ET, Winfrey MR (1987) Seasonal and Spatial Variations in Mercury Methylation and Demethylation in an Oligotrophic Lake. Appl Environ Microb 53:2397-2404.

Liu B, Yan HY, Wang CP, Li QH, Guedron S, Spangenberg JE, Feng XB, Dominik J (2012) Insights into low fish mercury bioaccumulation in a mercury-contaminated reservoir, Guizhou, China. Environ Pollut 160:109-117.

Loizeau J-L, Arbouille D, Santiago S, Vernet J-P (1994) Evaluation of a Wide-Range Laser Diffraction Grain-Size Analyzer for Use with Sediments. Sedimentology 41:353-361.

Loizeau J-L, Girardclos S, Dominik J (2012) Taux d'accumulation de sédiments récents et bilan de la matière particulaire dans le Léman (Suisse - France). Archives des Sciences 65:81-92.

Loizeau J-L, Makri S, Arpagaus Ph, Ferrari B, Casado-Martinez C, Benejam T, Marchand Ph (2017) Micropolluants métalliques et organiques dans les sédiments superficiels du Léman. Rapp Comm int prot eaux Léman contre pollut Campagne 2016, 143-198.

Marvin C, Charlton M, Milne J, Thiessen L, Schachtschneider G, Sverko E (2007) Metals associated with suspended sediments in Lakes Erie and Ontario, 2000-2002. Environ Monit Assess 130: 149-161.

Mason RP, Kim EH, Cornwell J, Heyes D (2006) An examination of the factors influencing the flux of mercury, methylmercury and other constituents from estuarine sediment. Mar Chem 102:96-110.

Mason RP, Choi AL, Fitzgerald WF, Hammerschmidt CR, Lamborg CH, Soerensen AL, Sunderland EM (2012) Mercury biogeochemical cycling in the ocean and policy implications. Environ Res 119:101-117.

OFEV (Editor) 2016: Annuaire hydrologique de la Suisse 2010. Office fédéral de l'environnement, Berne. Etat de l'environnement n° 1631: 627

Pardos M, Benninghoff C, De Alencastro LF, Wildi W (2004) The impact of a sewage treatment plant's effluent on sediment quality in a small bay in Lake Geneva (Switzerland–France). Part 1: Spatial distribution of contaminants and the potential for biological impacts. Lakes Reserv Res Manag 9: 41–52.

Parks JM, Johs A, Podar M, Bridou R, Hurt RA, Smith SD, Tomanicek SJ, Qian Y, Brown SD, Brandt CC, Palumbo AV, Smith JC, Wall JD, Elias DA, Liang LY (2013)

The Genetic Basis for Bacterial Mercury Methylation. Science 339:1332-1335.

Podar M, Gilmour CC, Brandt CC, Soren A, Brown SD, Crable BR, Palumbo AV, Somenahally AC, Elias DA (2015) Global prevalence and distribution of genes and microorganisms involved in mercury methylation. Sci Adv 1(9).

Pote J, Haller L, Loizeau J-L, Bravo AG, Sastre V, Wildi W (2008) Effects of a sewage treatment plant outlet pipe extension on the distribution of contaminants in the sediments of the Bay of Vidy, Lake Geneva, Switzerland. Bioresource Technol. 99:7122–7131.

Razmi AM, Barry DA, Bakhtyar R, Le Dantec N, Dastgheib A, Lemin U, Wüest A (2013) Current variability in a wide and open lacustrine embayment in Lake Geneva (Switzerland). J Great Lakes Res 39:455-465.

Rigaud S, Radakovitch O, Couture RM, Deflandre B, Cossa D, Garnier C, Garnier JM (2013) Mobility and fluxes of trace elements and nutrients at the sediment-water interface of a lagoon under contrasting water column oxygenation conditions. Appl Geochem 31:35-51.

Rolfhus KR, Sakamoto HE, Cleckner LB, Stoor RW, Babiarz CL, Back RC, Manolopoulos H, Hurley JP (2003) Distribution and fluxes of total and methylmercury in Lake Superior. Environ Sci Technol 37: 865-872.

Roos-Barraclough F, Givelet N, Martinez-Cortizas A, Goodsite ME, Biester H, Shotyk W (2002) An analytical protocol for the determination of total mercury concentrations in solid peat samples. Sci Total Environ 292:129-139.

Roos-Barraclough F, Shotyk W (2003) Millennial-scale records of atmospheric mercury deposition obtained from ombrotrophic and minerotrophic peatlands in the Swiss Jura Mountains. Environ Sci Technol 37:235-244.

Savoye L, Quetin P, Klein A (2015) Physico-chemical changes in the waters of Lake Geneva. Meteorological datas. Contributions from the tributaries of Lake Geneva and from the Rhone below Geneva Rapp Comm int prot eaux Léman contre pollut Campagne 2014,19-67.

Schartup AT, Ndu U, Balcom PH, Mason RP, Sunderland EM (2015) Contrasting Effects of Marine and Terrestrially Derived Dissolved Organic Matter on Mercury Speciation and Bioavailability in Seawater. Environ Sci Technol 49:5965-5972.

Taylor SE, Birch GF (2000) Contaminant dynamics in offchannel embayments of Port Jackson, New South Wales. A G S O 5-6:233-237.

Thevenon F, Graham ND, Chiaradia M, Arpagaus P, Wildi W, Pote J (2011) Local to regional scale industrial heavy metal pollution recorded in sediments of large freshwater lakes in central Europe (lakes Geneva and Lucerne) over the last centuries. Sci Total Environ 412:239-247.

Van Metre PC (2011) Increased atmospheric deposition of mercury in reference lakes near major urban areas. Environ Pollut 162:209-215.

Wang WX, Stupakoff I, Gagnon C, Fisher NS (1998) Bioavailability of inorganic and methylmercury to a marine deposit feeding polychaete. Environ Sci Technol 32:2564-2571.

Wiklund JA, Kirk JL, Muir DCG, Evans M, Yang F, Keating J, Parsons MT (2017) Anthropogenic mercury deposition in Flin Flon Manitoba and the Experimental Lakes Area Ontario (Canada): A multi-lake sediment core reconstruction. Sci Total Environ 586:685-695.

Supplementary information

Environmental Science and Pollution Research, 2018 (DOI :10.1007/s11356-018-2252-3)
Published online 16 May 2018

Total and methyl-mercury seasonal particulate fluxes in the water column of a large lake (Lake Geneva, Switzerland)

Elena Gascón Díez*, Neil D Graham‡, Jean-Luc Loizeau

Department F.-A. Forel for Environmental and Aquatic Sciences, and Institute for Environmental Sciences, University of Geneva, Boulevard Carl-Vogt 66, 1211 Geneva 4, Switzerland.

‡ present adress : *Soil & Water Research Infrastructure, Biology Centre, Czech Academy of Sciences, Na Sádkách 7, České Budějovice 370 05, Czech Republic*

* **Corresponding author** : Elena.Gascon@unige.ch

Table SI 1 : THg concentrations and fluxes at NG2 and NG3. Concentration errors correspond to one standard deviation determined from triplicate measurements. Errors on concentration and sediment accumulation rates are propagated to calculate flux uncertainties.

		NG2 Top Trap		**NG2 Bottom Trap**			**NG2 Sediment**
Date in dd/mm/yyyy	Date out	THg conc [μg/g]	THg flux [μg/m^2/day]	THg conc [μg/g]	THg flux [μg/m^2/day]	Core Sampling date	THg conc [μg/g]
09/12/2009	18/02/2010	0.22 ± 0.01	0.49 ± 0.01	0.21 ± 0.02	1.11 ± 0.01	26/01/2010	0.167 ± 0.005
18/02/2010	16/03/2010	0.18 ± 0.01	0.29 ± 0.01	0.23 ± 0.001	1.18 ± 0.01	18/02/2010	0.21 ± 0.01
16/03/2010	08/04/2010	0.17 ± 0.01	0.24 ± 0.02	0.21 ± 0.01	0.80 ± 0.04	16/03/2010	0.23 ± 0.02
08/04/2010	07/05/2010	0.106 ± 0.004	0.49 ± 0.02	0.22 ± 0.04	1.6 ± 0.3	08/04/2010	0.189 ± 0.003
07/05/2010	02/06/2010	0.13 ± 0.01	0.57 ± 0.03	0.142 ± 0.001	0.82 ± 0.01	07/05/2010	0.178 ± 0.005
02/06/2010	29/06/2010	0.13 ± 0.01	1.13 ± 0.06	0.142 ± 0.001	1.36 ± 0.01	02/06/2010	0.18 ± 0.02
29/06/2010	20/09/2010	0.073 ± 0.001	0.58 ± 0.01	0.074 ± 0.001	0.72 ± 0.01	29/06/2010	0.20 ± 0.02
29/09/2010	05/11/2010	0.24 ± 0.01	0.87 ± 0.03	0.20 ± 0.01	1.01 ± 0.06	16/09/2010	0.174 ± 0.002
05/11/2010	10/12/2010	0.24 ± 0.06	1.1 ± 0.3	0.23 ± 0.04	1.0 ± 0.2	10/12/2010	0.235 ± 0.009
14/12/2010	04/01/2011	0.27 ± 0.01	1.90 ± 0.07	0.26 ± 0.01	3.0 ± 0.1	04/01/2011	0.186 ± 0.004
04/01/2011	02/02/2011	0.136 ± 0.002	0.15 ± 0.01	0.202 ± 0.01	0.66 ± 0.02	02/02/2011	0.204 ± 0.004
02/02/2011	09/03/2011	0.174 ± 0.002	0.14 ± 0.01	0.218 ± 0.01	0.64 ± 0.02	09/03/2011	0.18 ± 0.01
09/03/2011	06/04/2011	0.19 ± 0.04	0.7 ± 0.2	0.197 ± 0.002	1.00 ± 0.01	06/04/2011	0.19 ± 0.01
06/04/2011	03/05/2011	0.17 ± 0.02	0.59 ± 0.08	0.10 ± 0.02	0.5 ± 0.1	03/05/2011	0.20 ± 0.02
03/05/2011	27/06/2011	0.08 ± 0.02	0.21 ± 0.05	0.10 ± 0.01	0.27 ± 0.01	27/06/2011	0.20 ± 0.03
27/06/2011	23/07/2011	0.11 ± 0.03	0.8 ± 0.2	0.073 ± 0.002	0.49 ± 0.02	23/07/2011	0.18 ± 0.01
23/07/2011	10/08/2011	0.08 ± 0.01	0.56 ± 0.09	0.07 ± 0.01	0.55 ± 0.01	10/08/2011	0.25 ± 0.08
10/08/2011	11/09/2011	0.083 ± 0.001	1.22 ± 0.01	0.084 ± 0.01	1.27 ± 0.08	21/09/2011	0.27 ± 0.06
		NG3 Top Trap		**NG3 Bottom Trap**			**NG3 Sediment**
Date in	Date out	THg conc [μg/g]	THg flux [μg/m^2/day]	THg conc [μg/g]	THg flux [μg/m^2/day]	Core Sampling date	THg conc [μg/g]
18/02/2010	16/03/2010	0.140 ± 0.002	0.131 ± 0.002	0.214 ± 0.008	0.94 ± 0.03	16/03/2010	0.19 ± 0.02
16/03/2010	08/04/2010	0.152 ± 0.001	0.166 ± 0.001	0.211 ± 0.015	0.77 ± 0.05	08/04/2010	0.22 ± 0.02
08/04/2010	07/05/2010	0.057 ± 0.004	0.19 ± 0.02	0.126 ± 0.004	0.67 ± 0.02	07/05/2010	0.20 ± 0.02
07/05/2010	02/06/2010	0.074 ± 0.002	0.221 ± 0.006	0.097 ± 0.003	0.37 ± 0.01	02/06/2010	0.194 ± 0.006
02/06/2010	29/06/2010	0.074 ± 0.002	0.42 ± 0.01	0.097 ± 0.003	0.58 ± 0.02	29/06/2010	0.171 ± 0.002
29/06/2010	20/09/2010	0.038 ± 0.001	0.233 ± 0.002	0.057 ± 0.001	0.39 ± 0.01	20/09/2010	0.265 ± 0.001
29/09/2010	10/12/2010	0.146 ± 0.004	0.33 ± 0.01	0.20 ± 0.07	0.6 ± 0.2	10/12/2010	0.253 ± 0.005
14/12/2010	04/01/2011	0.169 ± 0.003	0.56 ± 0.01	0.20 ± 0.01	1.32 ± 0.08	04/01/2011	0.248 ± 0.007
04/01/2011	02/02/2011	0.16 ± 0.02	0.13 ± 0.01	0.170 ± 0.004	0.39 ± 0.01	02/02/2011	0.203 ± 0.004
02/02/2011	09/03/2011	0.152 ± 0.008	0.097 ± 0.005	0.193 ± 0.002	0.60 ± 0.01	09/03/2011	0.166 ± 0.002
09/03/2011	06/04/2011	0.11 ± 0.01	0.38 ± 0.04	0.177 ± 0.005	0.89 ± 0.02	06/04/2011	0.248 ± 0.005
06/04/2011	31/05/2011	0.059 ± 0.004	0.102 ± 0.008	0.097 ± 0.004	0.27 ± 0.01	03/05/2011	0.206 ± 0.007
31/05/2011	27/06/2011	0.060 ± 0.005	0.15 ± 0.01	0.086 ± 0.001	0.20 ± 0.01	27/06/2011	0.182 ± 0.002
27/06/2011	23/07/2011	0.041 ± 0.001	0.238 ± 0.008	0.059 ± 0.001	0.30 ± 0.01	23/07/2011	0.201 ± 0.003
23/07/2011	10/08/2011	0.053 ± 0.001	0.281 ± 0.008	0.064 ± 0.001	0.37 ± 0.01	10/08/2011	0.224 ± 0.003
10/08/2011	11/09/2011	0.047 ± 0.001	0.517 ± 0.007	0.055 ± 0.002	0.52 ± 0.02	09/09/2011	0.229 ± 0.002

Table SI 2 : MeHg concentrations and fluxes at NG2 and NG3. Concentration errors correspond to one standard deviation determined from triplicate measurements. Errors on concentration and sediment accumulation rates are propagated to calculate uncertainties on fluxes.

		NG2 Top Trap		**NG2 Bottom Trap**			**NG2 Sediment**
Date in	Date out	MeHg conc [ng/g]	MeHg flux [ng/m^2/day]	MeHg conc [ng/g]	MeHg flux [ng/m^2/day]	Core Sampling date	MeHg conc [ng/g]
09/12/2009	18/02/2010	2.69 ± 0.05	6.1 ± 0.1	8.91 ± 0.05	47.6 ± 0.3	18/02/2010	0.31 ± 0.05
18/02/2010	16/03/2010	1.44 ± 0.03	2.29 ± 0.04	0.74 ± 0.02	3.8 ± 0.1	16/03/2010	1.24 ± 0.01
16/03/2010	08/04/2010	1.32 ± 0.09	1.9 ± 0.1	1.07 ± 0.02	4.2 ± 0.1	08/04/2010	0.70 ± 0.03
08/04/2010	07/05/2010	1.9 ± 0.4	9 ± 2	5.31 ± 0.03	37.0 ± 0.3	07/05/2010	1.42 ± 0.01
07/05/2010	02/06/2010	1.7 ± 0.2	8 ± 1	6.10 ± 0.03	35.1 ± 0.2	02/06/2010	0.81 ± 0.01
02/06/2010	29/06/2010	2.7 ± 0.2	23 ± 2	4.19 ± 0.03	40.0 ± 0.3	29/06/2010	0.87 ± 0.03
29/06/2010	20/09/2010	9 ± 1	68 ± 8	3.35 ± 0.02	33.0 ± 0.2	20/09/2010	0.31 ± 0.03
29/09/2010	05/11/2010	6.3 ± 0.1	23.4 ± 0.1	11.38 ± 0.02	55.9 ± 0.2	27/10/2010	1.67 ± 0.02
05/11/2010	10/12/2010	2.0 ± 0.3	9 ± 2	1.5 ± 0.2	6.6 ± 0.7	10/12/2010	1.31 ± 0.09
14/12/2010	04/01/2011	0.55 ± 0.03	3.9 ± 0.2	2.78 ± 0.01	32.3 ± 0.2	04/01/2011	0.87 ± 0.01
04/01/2011	02/02/2011	0.41 ± 0.04	0.44 ± 0.04	0.83 ± 0.01	2.72 ± 0.04	02/02/2011	0.89 ± 0.07
02/02/2011	09/03/2011	4.58 ± 0.01	3.79 ± 0.01	1.77 ± 0.01	5.21 ± 0.03	09/03/2011	0.72 ± 0.01
09/03/2011	06/04/2011	3.83 ± 0.01	14.9 ± 0.1	4.21 ± 0.01	21.5 ± 0.1	06/04/2011	1.08 ± 0.03
06/04/2011	03/05/2011	1.00 ± 0.03	3.5 ± 0.1	2.00 ± 0.03	10.2 ± 0.2	03/05/2011	0.71 ± 0.03
03/05/2011	27/06/2011	10.43 ± 0.01	25.95 ± 0.1	2.44 ± 0.01	6.68 ± 0.02	27/06/2011	0.491 ± 0.004
27/06/2011	23/07/2011	4.25 ± 0.01	30.6 ± 0.1	6.65 ± 0.003	46.4 ± 0.1	23/07/2011	0.613 ± 0.004
23/07/2011	10/08/2011	6.93 ± 0.02	49.1 ± 0.3	4.14 ± 0.02	31.1 ± 0.2	10/08/2011	1.43 ± 0.02
10/08/2011	11/09/2011	0.67 ± 0.04	9.8 ± 0.6	0.62 ± 0.04	9.5 ± 0.6	09/09/2011	0.81 ± 0.01
		NG3 Top Trap		**NG3 Bottom Trap**			**NG3 Sediment**
Date in	Date out	MeHg conc [ng/g]	MeHg flux [ng/m^2/day]	MeHg conc [ng/g]	MeHg flux [ng/m^2/day]	Core Sampling date	MeHg conc ng/g]
						18/02/2010	0.84 ± 0.05
18/02/2010	16/03/2010	0.99 ± 0.02	0.93 ± 0.02	0.46 ± 0.02	2.0 ± 0.1	16/03/2010	1.24 ± 0.03
16/03/2010	08/04/2010	1.39 ± 0.02	1.51 ± 0.02	0.39 ± 0.02	1.43 ± 0.08	08/04/2010	0.21 ± 0.02
08/04/2010	07/05/2010	2.42 ± 0.01	8.28 ± 0.04	3.52 ± 0.01	18.76 ± 0.06	07/05/2010	0.49 ± 0.01
07/05/2010	02/06/2010	1.06 ± 0.03	3.2 ± 0.1	1.31 ± 0.03	4.9 ± 0.1	02/06/2010	0.27 ± 0.01
02/06/2010	29/06/2010	1.92 ± 0.03	11.0 ± 0.2	2.92 ± 0.03	17.4 ± 0.2	29/06/2010	0.75 ± 0.03
29/06/2010	20/09/2010	4.89 ± 0.02	29.6 ± 0.1	8.52 ± 0.03	58.5 ± 0.2	20/09/2010	0.87 ± 0.02
29/09/2010	10/12/2010	1.4 ± 0.2	3.2 ± 0.3	13.5 ± 0.2	42.3 ± 0.5	27/11/2010	1.49 ± 0.02
14/12/2010	04/01/2011	1.22 ± 0.01	4.09 ± 0.03	1.11 ± 0.01	7.51 ± 0.06	10/12/2010	0.98 ± 0.09
04/01/2011	02/02/2011	0.87 ± 0.01	0.71 ± 0.01	0.95 ± 0.01	2.16 ± 0.03	04/01/2011	0.77 ± 0.01
02/02/2011	09/03/2011	1.0 ± 0.01	0.68 ± 0.01	1.02 ± 0.01	3.19 ± 0.03	02/02/2011	18.71 ± 0.07
09/03/2011	06/04/2011	2.55 ± 0.01	8.68 ± 0.04	2.06 ± 0.01	10.45 ± 0.06	09/03/2011	0.59 ± 0.01
06/04/2011	31/05/2011	5.86 ± 0.03	10.05 ± 0.05	12.74 ± 0.03	34.93 ± 0.09	06/04/2011	0.81 ± 0.03
31/05/2011	27/06/2011	7.25 ± 0.01	18.14 ± 0.02	8.88 ± 0.01	20.26 ± 0.03	03/05/2011	0.73 ± 0.03
27/06/2011	23/07/2011	3.90 ± 0.01	22.47 ± 0.02	2.28 ± 0.01	11.53 ± 0.02	27/06/2011	0.609 ± 0.004
23/07/2011	10/08/2011	7.09 ± 0.01	37.35 ± 0.08	6.92 ± 0.01	40.18 ± 0.08	23/07/2011	0.138 ± 0.003
10/08/2011	11/09/2011	1.80 ± 0.04	20.0 ± 0.4	2.35 ± 0.04	22.2 ± 0.4	10/08/2011	2.28 ± 0.02
						09/09/2011	0.12 ± 0.01

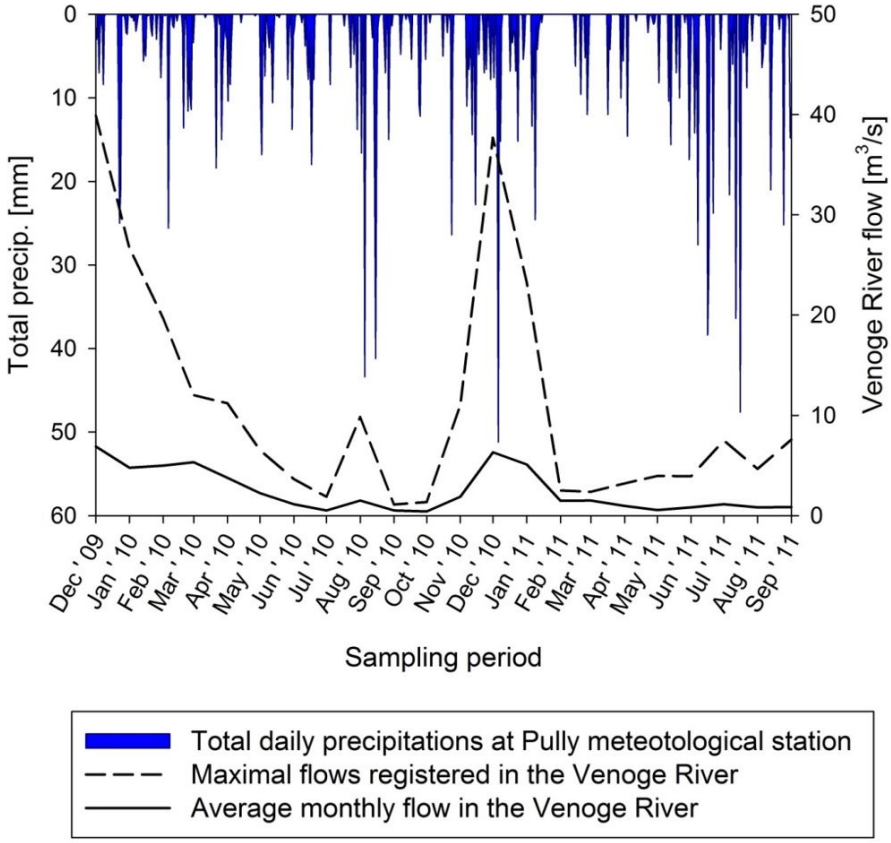

Figure SI 1 : Total daily precipitation measured at the Pully weather station, coupled with the maximum and average flows of the Venoge River, tributary of Lake Geneva, in the vicinity of Vidy Bay. Data collected from http ://www.agrometeo.ch/fr/meteorology/datas and http ://www.hydrodaten.admin.ch/fr/2432.html